the only observed product. In the condensed phase the $Re_2(CO)_{9,10}^-$ is thought to extract a proton from the solvent, ethanol. In the gas phase $Re_2(CO)_9^-$ does not extract a proton from alcohols. Ethanol may be a stronger acid toward $Re_2(CO)_9^-$ in condensed phase because the conjugate base, $C_2H_5O^-$, is very effectively solvated in protic solvents.

The proton affinities of the dimetal decacarbonyls increase slightly on going from $Mn_2(CO)_{10}$ to $ReMn(CO)_{10}$ to $Re_2(CO)_{10}$. Substituting a methyl group for $Re(CO)_5$ or $Mn(CO)_5$ has only small effects. The hydrogen atom is probably bonded terminally to one of the metals in the protonated $M_2CO)_{10}$ species.

Acknowledgment. We thank Professor Andrew Wojcicki, who kindly provided the sample of $ReMn(CO)_{10}$, and the National Science Foundation for partial support of this research under Grant CHE 81-10516.

Registry No. $Mn_2(CO)_{10}$, 10170-69-1; $ReMn(CO)_{10}$, 14693-30-2; $Re_2(CO)_{10}$, 14285-68-8.

Vibrational Circular Dichroism of *trans*-1,2-Dideuteriocyclobutane. Experimental and Calculational Results in the Mid-Infrared

A. Annamalai,[†] T. A. Keiderling,*[†] and J. S. Chickos[‡]

Contribution from the Departments of Chemistry, University of Illinois at Chicago, Chicago, Illinois 60680, and University of Missouri—St. Louis, St. Louis, Missouri 63121.
Received August 3, 1984

Abstract: We have measured the VCD of *trans*-1,2-dideuteriocyclobutane in the mid-IR and have compared it to the results of fixed partial charge and localized molecular orbital calculations. For a force field optimized from the ab initio results of Banhegyi et al., we find good agreement between calculated and experimental results for the FPC but not for the LMO model. Other force fields and charge configurations were also investigated with the general result that optimized force fields gave superior results due to better representation of both the modes and their frequency distributions.

In recent years vibrational circular dichroism (VCD) has become technologically feasible in the near- and mid-IR.[1,2] The utility of such measurements is dependent on the development of theoretical models which can reliably represent the relationship between VCD spectra and molecular structure. Two such models, the fixed partial charge[3] (FPC) and localized molecular orbital[4] (LMO) models, have proven to be calculationally useful in several recent studies which compared calculations with experimental VCD spectra in the near-IR region[5] ($\nu > 2000$ cm^{-1}). We have recently analyzed these two models in detail with respect to their ability to reproduce the C–H and C–D stretching VCD of *trans*-1,2-dideuteriocyclobutane.[6] These results indicated that both models gave qualitatively the same VCD but did differ in the order of magnitude of the predicted VCD. However, the $\Delta A/A$ ratios calculated were about the same with each model. The major factor that we found to be necessary in that work for good agreement with experiment was the obtaining of a force field which correctly reproduced the relative frequency spacings of the overlapped modes. The various force fields we used did not significantly alter the calculated rotational strengths of individual stretching modes but did alter their interfering VCD overlap. Our best results were obtained with a new force field derived from the ab initio results of Banhegyi, Fogarasi, and Pulay[7] (hereafter BFP) by optimizing to best reproduce the frequencies of several isotopomers.[8]

Cyclobutane has several advantages for such a comparative test of theoretical models. Its small size, lack of heteroatoms, and known geometry[9] combine to simplify calculational work. Furthermore, the force fields that are now available, refined to fit the isotopic variants,[8] provide a necessary ingredient for both models.[3,4] We have previously reviewed the successes and failures of the FPC and LMO models.[6] In short, it is clear that the C–H and C–D stretching modes of a pure hydrocarbon should provide a best possible case for both. The presence of two conformers in *trans*-1,2-dideuteriocyclobutane (with deuteriums equatorial or axial to the ring) additionally provides some cancellation of coupled-oscillator-type effects that are thought to dominate VCD of previously analyzed six-member ring systems.[10] This coupling will occur between all pairs of local oscillators[11] and can give rise to significant VCD when the transition dipole moments are large and the modes involved are strongly coupled.[12]

[†] University of Illinois at Chicago.
[‡] University of Missouri—St. Louis.

(1) For reviews of VCD see: Nafie, L. A. In "Advances in Infrared and Raman Spectroscopy"; Clark, R. J. H., Hester, R. E., Eds.; Heydon: London, 1984: Vol 11. Nafie, L. A. In "Vibrational Spectra and Structure"; Durig, J. R., Ed.; Elsevier: New York, 1981; Vol 10. Nafie, L. A.; Diem, M. *Acc. Chem. Res.* **1979**, *12*, 296. Stephens, P. J.; Clark, R. In "Optical Activity and Chiral Descrimination"; Mason, S. F., Ed.; Reidel: Dortrecht, 1979. Mason, S. F. In "Advances in Infrared and Raman Spectroscopy"; Clark, R. J. H.; Hester, R. E., Eds.; Heyden: London, 1980; Vol 8. Polavarapu, P. L. In "Vibrational Spectra and Structure"; Durig, J. R., Ed.; Elsevier: New York, 1984; Vol 13.
(2) Keiderling, T. A. *Appl. Spectrosc. Rev.* **1981**, *17*, 189.
(3) Schellman, J. A. *J. Chem. Phys.* **1973**, *58*, 2882; **1974**, *6*, 343.
(4) Nafie, L. A.; Walnut, T. H. *Chem. Phys. Lett.* **1977**, *49*, 441. Walnut, T. H.; Nafie, L. A. *J. Chem. Phys.* **1977**, *67*, 1501. Nafie, L. A.; Polavarapu, P. L. *J. Chem. Phys.* **1981**, *75*, 2935.
(5) Polavarapu, P. L.; Nafie, L. A. *J. Chem. Phys.* **1981**, *75*, 2945. Keiderling, T. A.; Stephens, P. J. *J. Am. Chem. Soc.* **1979**, *101*, 1396. Singh, R. D.; Keiderling, T. A. *J. Chem. Phys.* **1981**, *74*, 5347; *J. Am. Chem. Soc.* **1981**, *103*, 2387. Polavarapu, P. L.; Nafie, L. A. *J. Chem. Phys.* **1980**, *73*, 1567. Marcott, C.; Scanlon, K.; Overend, J.; Moscowitz, A. *J. Am. Chem. Soc.* **1981**, *103*, 483. Freedman, T. B.; Diem, M.; Polavarapu, P. L.; Nafie, L. A. *J. Am. Chem. Soc.* **1982**, *104*, 3343.
(6) Annamalai, A.; Keiderling, T. A.; Chickos, J. S. *J. Am Chem. Soc.* **1984**, *106*, 6254.
(7) Banhegyi, G.; Fogarasi, G.; Pulay, P. *J. Mol. Struct.* **1982**, *89*, 1.
(8) Annamalai, A.; Keiderling, T. A. *J. Spectrosc.* **1985**, *109*, 46.
(9) Skancke, P. N.; Fogarasi, G.; Boggs, J. E. *J. Mol. Struct.* **1980**, *62*, 259. Cremer, D. *J. Am. Chem.* Soc. **1977**, *99*, 1307. Meiboom, S.; Snyder, L. C. *J. Am. Chem. Soc.* **1967**, *89*, 1038; *J. Chem. Phys.* **1970**, *52*, 3857.
(10) Laux, L.; Pultz, V.; Abbate, S.; Havel, H. A.; Overend, J. A.; Moscowitz, A.; Lightner, D. A. *J. Am. Chem. Soc.* **1982**, *104*, 4276.
(11) Holzwarth, G.; Chabay, I. *J. Chem. Phys.* **1972**, *57*, 1632.
(12) Narayanan, U.; Keiderling, T. A. J. *Am. Chem. Soc.* **1983**, *105*, 6406. Su, C. N.; Keiderling, T. A. *J. Am. Chem. Soc.* **1980**, *102*, 511.

0002-7863/85/1507-2285$01.50/0

In this paper, we report the results of our mid-IR VCD measurements on *trans*-1,2-dideuteriocyclobutane in both vapor and solution phases and compare them with the FPC and LMO calculated spectra. Such a comparison is of interest because FPC calculations are much cheaper and easier to use than LMO. Hence, identification of molecular systems for which the FPC model is both applicable and useful would be of great help for analysis of VCD. To our knowledge, the calculations presented here represent the first reported comparison of such results to mid-IR VCD. The mid-IR poses a significant difference from the more often studied C–H stretching region VCD. Here normal modes are not only overlapped in frequency but the various internal coordinates are often strongly coupled via the force field. Hence, we might expect and, indeed, find a stronger dependence on the force field than seen for the C–H and C–D stretching regions.[6] Also, since lower energy, framework vibrations of the molecules are involved, one might expect significant differences to be found between the FPC and LMO models.

Experimental Section

All samples used were prepared and purified at the University of Missouri, St. Louis, as summarized in our previous paper.[6] VCD and infrared absorption measurements were made on the University of Illinois at Chicago instrument[2] with use of both gas and solution cells of our own design for handling the volatile cyclobutane.[6] In particular, the gas cell had a 7 cm path length with NaCl windows while the solution cell had a 8 mm path with BaF_2 windows. These latter windows plus the CS_2-solvent absorption conspired to limit solution studies to the 1360–930 cm^{-1} region while the vapor-phase measurements were made for the 1560–850 cm^{-1} region. Additional solution studies in different solvents were not possible due to lack of sample. Instrumentation modifications to enable VCD measurements in the mid-IR have been detailed elsewhere.[13]

The pressure in the gas cell and the ϵ and $\Delta\epsilon$ values have been estimated from the mass of the sample condensed from a vacuum line to fill the cell and from its volume. The concentrations of the solution samples are unknown due to the difficulty in accurately filling this cell with both solute and solvent. The solution spectra are thus represented only in terms of A and ΔA. Because of the very low extinction coefficient of cyclobutane in the mid-IR, it was necessary to employ relatively large amounts of optically active isomer (~65 mg for the vapor-phase study). Due to availability restrictions, we were forced to use a sample of (1*S*,2*S*) isomer that was only 70% enantiomerically pure. The plotted data presented here have been both corrected for this and converted to be appropriate for the (1*R*,2*R*) isomer for the ease of comparison with our previous results.[6]

For the vapor-phase experiment, a racemic sample was used to obtain the VCD base line. Additionally, N_2 flushing was used to minimize the effects of atmospheric water vapor. In the solution experiments, only a CS_2-solvent-filled cell was used for the VCD base line. This, as well as several experimental difficulties which led to some drift of the instrumental base line in the course of the measurement, leads us to believe that the solution spectra are less quantitatively reliable than are the vapor spectra. Due to the loss of rotational structure, the solution absorption spectrum has higher extinctions (at the 4 to 9 cm^{-1} resolution used) and consequently less sample was used for VCD. Since the VCD was not correspondingly sharper, the signal-to-noise ratio also deteriorated for this sample. Data from two separate runs with different sample concentrations are joined together to get the best possible spectrum.

Calculations

The calculational methods and force fields employed have been fully described previously,[6] and details of our normal coordinate analysis of *trans*- and *cis*-1,2-dideuteriocyclobutanes are published separately.[8] The lettering scheme used to indicate different force fields that we used in our previous work will be maintained here for the ease of comparison. In particular, A implies the force field of Lord and Nakagawa[14] (L&N), B our optimization of A for the puckered geometry,[9] C the BFP ab initio force field,[7] and D our optimization of C.[8]

Two charge distributions were investigated for the FPC calculations. As before,[6] we used empirical charges of −0.28 |e| on C and +0.14 |e| on H(D), derived by fitting the integrated C–H and C–D stretching absorption intensity, as well as CNDO charges with −0.0189 |e| on C, +0.0171 |e| on equatorial H(D), and +0.0018 |e| on axial H(D) atoms. In these latter charges, one can notice the significant difference between the equatorial and axial hydrogens and much smaller magnitudes than the empirical ones. Since neither set of charges was optimized for the mid-IR, we did not expect them to quantitatively reproduce the mid-IR intensities.

Finally, the FPC calculations were done with a modification[6] of Schachtschneider's GMAT and FPERT programs[15] while the LMO calculations were carried out with the finite nuclear displacement method with CNDO based programs kindly provided to us by Dr. P. L. Polavarapu.[16] These schemes used the standard formulations of Schellman for FPC[3] and those of Nafie and Polavarapu for LMO[4] calculations.

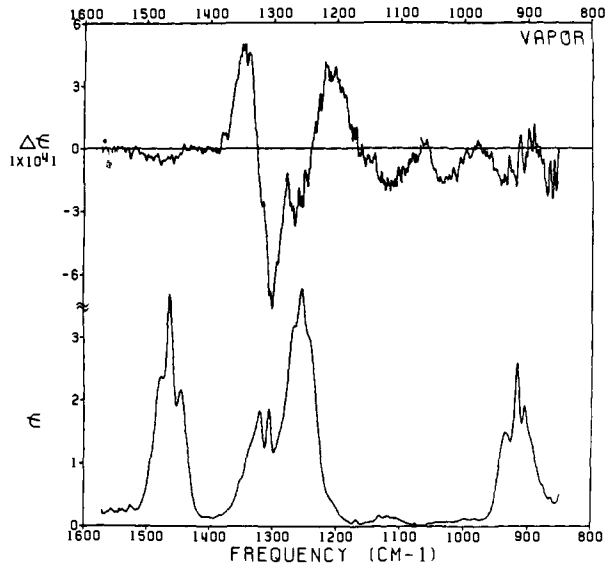

Figure 1. Experimental gas-phase VCD and absorption spectra of *trans*-1,2-dideuteriocyclobutane in the mid-IR, measured for partially resolved (1*S*,2*S*) isomer but presented for fully resolved (1*R*,2*R*) isomer. Pressure, ~360 torr; path length, 7 cm; time constant, 3 s; average of 6 scans; resolution varies from 9 to 4 cm^{-1} for 1560–1070 cm^{-1} and from 7 to 4 cm^{-1} for 1070–850 cm^{-1}. The 1560–1400 cm^{-1} region was scanned with N_2 flushing of the instrument.

Results

In Figure 1 are shown the mid-IR VCD and absorption spectra of *trans*-(1*R*,2*R*)-dideuteriocyclobutane in the gas phase. The effect of the low resolution used (~4 to 9 cm^{-1}) is apparent by comparison with our FTIR results[8] which show sharper, more intense Q branches than seen here at ~1450, 1315, 1250, and 900 cm^{-1}. Our attempts to measure VCD of the relatively isolated 900-cm^{-1} band gave $\Delta A/A \leq 3 \times 10^{-5}$ (i.e., approximately equal to the noise level). Similarly, the 1450-cm^{-1}-region CH_2 scissor modes give only a small negative VCD. The 1350–1200 cm^{-1} region evidences at least three overlapping bands in absorption. However, the VCD here is strong and has four clear features which do not correspond to the largest absorption features. In particular, the large positive peak at 1340 cm^{-1} (vapor phase) correlates with a shoulder as does the other positive band at 1210 cm^{-1}. The weak absorptions in the 1180–980 cm^{-1} region yield two relatively large VCD features.

In the region where they overlap, the solution VCD spectrum (Figure 2) has the same structure as the vapor spectrum. The major differences between the two are a slight increase in resolution, due to collapse of rotational structure; some shifts in frequencies; and an increase in noise for the solution spectrum. CS_2 absorption prevented the study of the 1450-cm^{-1} band. Contrary to the C–H stretching results,[6] no increase in $\Delta A/A$ values was found for the solution as compared to the vapor-phase mid-IR results. The 1250-cm^{-1} VCD band does appear to be much

(13) Su, C. N.; Heintz, V. J.; Keiderling, T. A. *Chem. Phys. Lett.* **1980**, *73*, 157. Heintz, V. J.; Freeman, W. A.; Keiderling, T. A. *Inorg. Chem.* **1983**, *22*, 2319.

(14) Lord, R. C.; Nakagawa, I. *J. Chem. Phys.* **1963**, *39*, 2951.

(15) Schachtschneider, J. H., Technical Report No. 231-64, 1964; 57-65, 1965, Shell Development Co., California.

(16) Polavarapu, P. L. *J. Chem. Phys.* **1982**, *72*, 2273. Polavarapu, P. L.; Chandrasekhar, J. *Chem. Phys. Lett.* **1981**, *84*, 587. Nafie, L. A.; Freedman, T. B. *J. Chem. Phys.* **1981**, *75*, 4847.

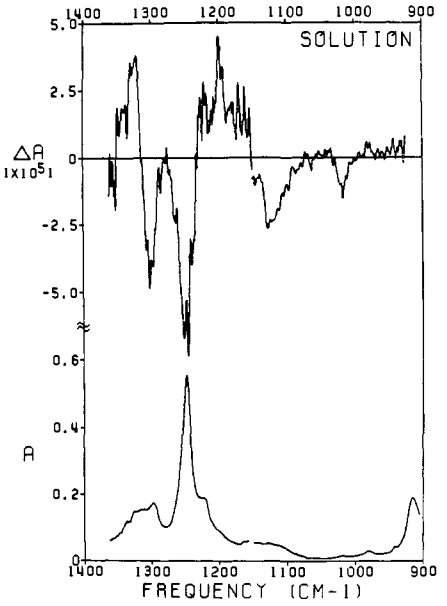

Figure 2. Experimental CS_2 solution-phase VCD and absorption spectra in the mid-IR. Concentration is unknown; path length, 8 mm. Measurement conditions are as in Figure 1 except that the resolution change is at 1150 cm^{-1}.

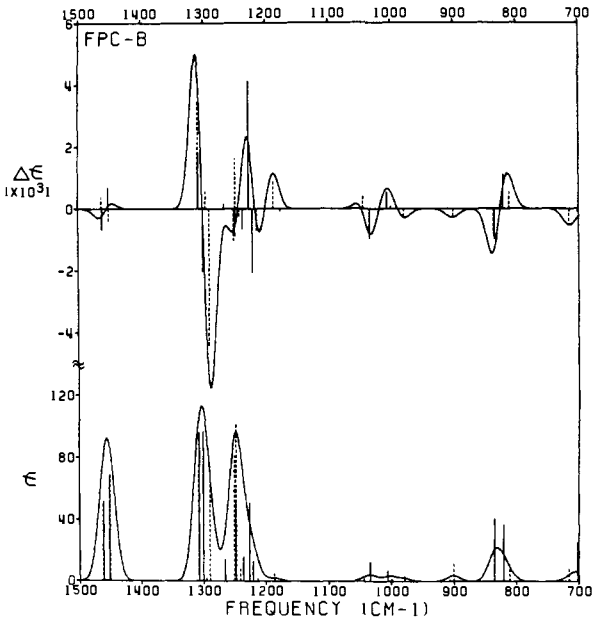

Figure 3. Calculated VCD and absorption spectra in the mid-IR with the FPC model and force field B. Dashed vertical lines indicate the axial conformer and solid vertical lines the equatorial conformer contributions to the overall line shape. Plots were made with 15 cm^{-1} line width Gaussians centered at the normal mode frequencies and 50% of the sum of $\Delta\epsilon$ and ϵ values for the axial and equatorial conformers.

larger, relative to the other bands, in the solution spectrum. Due to base line limitations mentioned above, we would not attempt to interpret this. This band, being sharp and the most intense, is the one most likely to be distorted by artifacts in our instrument.

Our initial calculations (FPC-A) used the L&N force field[14] directly. These calculations gave frequency deviations from experiment as large as 50 cm^{-1} for the major absorption peaks and showed only slight resemblance to the observed dideuteriocyclobutane absorption and VCD spectra. Upon conventional refinement of this force field for D_{2d} geometry with a revised C_4H_8 and C_4D_8 frequency assignment,[17] the results FPC-B were obtained. These two calculations are compared in Table I for both conformers. The FPC-B results, presented graphically in Figure 3, distinctly show the major patterns seen in the experimental spectrum. The vertical lines drawn under the Gaussian broadened (15 cm^{-1}) line shape emphasize the contributions both of individual modes and of the two different conformers (dashed lines indicate the conformer with axially substituted deuterium and solid lines those substituted equatorially). The major features in the experimental spectrum are seen in the FPC-B calculated results with only the calculated band at 1185 cm^{-1} being unaccounted for. The 1450-cm^{-1} region is indicated to have only a weak couplet due to cancellation of oppositely signed coupled oscillator effects in each conformer, which is consistent with the weak VCD found. Furthermore, the two major positive VCD features correlate with shoulders (or tails) of strong absorption bands. The 1320-cm^{-1} VCD band is the high-energy half of a couplet, corresponding to CDH scissor-like modes, having the same sense in each conformer.

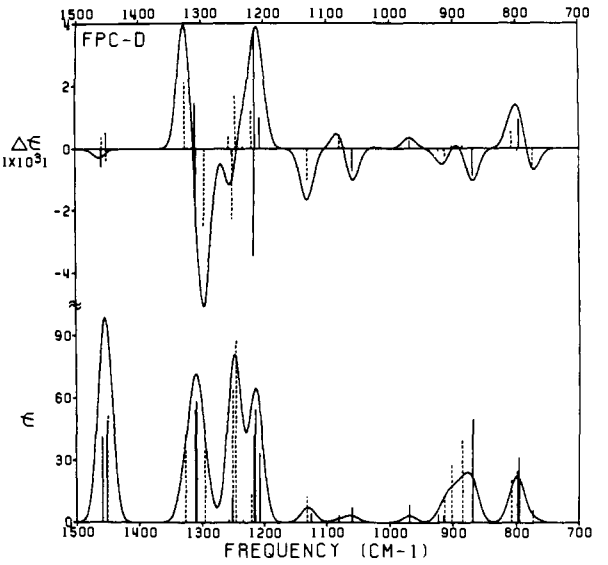

Figure 4. As in Figure 3 except with FPC-D, for the force field optimized from the BFP ab initio force field.

We next calculated the VCD with the BFP force field (FPC-C) and then with our frequency fitted force field[8] (FPC-D) which started from the BFP force constants. These results are compared in Table II, and those of FPC-D are graphically shown in Figure 4. The FPC-C spectrum gives a somewhat better picture of the experimental VCD than does FPC-B, but the FPC-D (Figure 4) yields the best agreement with the signs, shapes, and relative magnitudes of the experimental spectrum. The major difference between the FPC-B and FPC-D results is a general spread of the calculated frequencies due to the increased number and influence of the interaction constants in the latter force field. Again, in FPC-D, the main features of the experimental VCD are reproduced; however, in this case, the calculated absorption spectrum has too much intensity at 1220 cm^{-1}, i.e., what should be a shoulder that correlates to strong positive VCD is now evidenced as a peak. If the two calculated bands at 1250 and 1220 cm^{-1} had overlapped more, a better representation of the experimental spectrum would result.

In an effort to understand better the dependence of charge configuration, we also calculated the FPC-D VCD with charges obtained from the CNDO population analysis.[18] These results are represented graphically in Figure 5. Unlike the C–H stretching region, here we find differences in both the absorption and VCD from the empirical charge results. But, except for the region around 930 cm^{-1}, where we have little data, the changes are only ones of relative magnitudes, and the general shape is preserved. Contrary to our previous results,[6] the CNDO charge set gives a slightly better representation of the absorption pattern.

(17) Miller, F. A.; Capwell, R. J.; Lord, R. C.; Rea, D. G. *Spectrochim. Acta* **1972**, *28A*, 603. Rea, D. G. Ph.D. Thesis, Massachusetts Institute of Technology, 1954.

(18) Pople, J. A.; Beveridge, D. L. "Approximate Molecular Orbital Theory"; McGraw-Hill, New York, 1970.

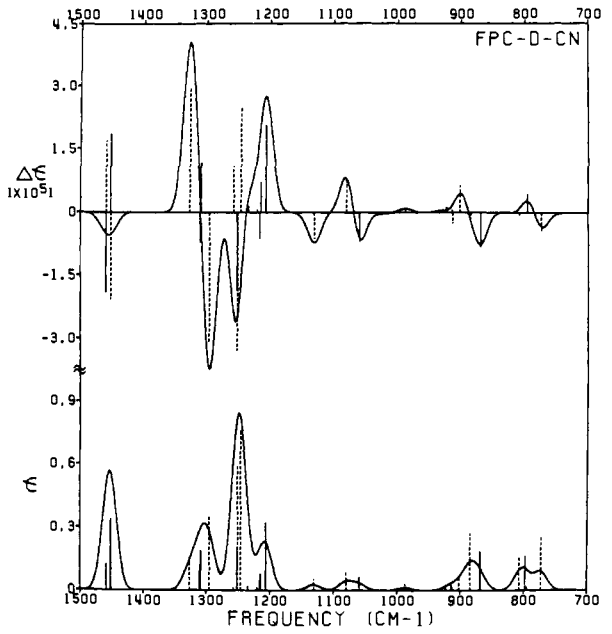

Figure 5. As in Figure 4 except with the charges derived from CNDO calculations.

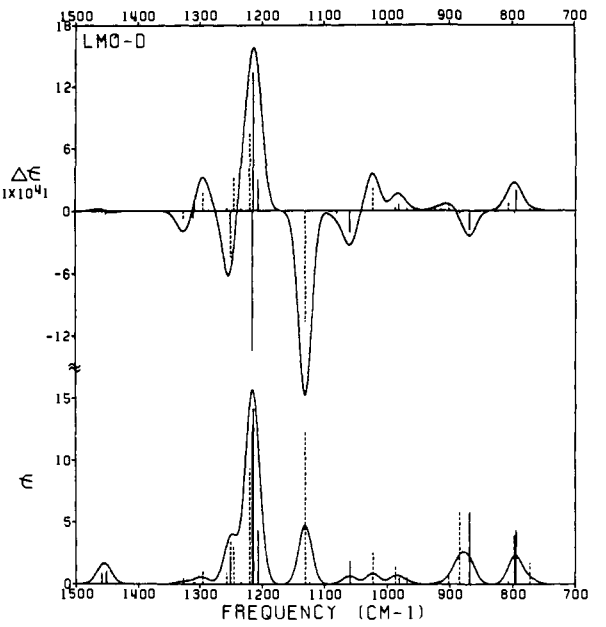

Figure 6. As in Figure 4 except with LMO-D results.

In the FPC calculated spectra above, the empirical charges carried over from our C–H region study yield VCD and absorption that is much too intense. Calculated extinction coefficients are ~20 times too large in FPC-D, the best case. Unscaled CNDO charges, however, give results somewhat smaller than those found in experiment but in better agreement. $\Delta\epsilon/\epsilon$ values calculated in the FPC scheme appear to be generally somewhat smaller than the experimental ones, but the lack of alignment between the VCD and absorption makes such comparisons very difficult.

Given these qualitatively satisfying results obtained above with the simple FPC model, an attempt was made to compare similarly calculated LMO results. Such calculations were made for both of our optimized force fields, B (Table I) and D (Table II). Unlike our C–H stretching VCD calculations, the LMO and FPC spectra differed both qualitatively and quantitatively in the mid-IR.

The LMO-D results, i.e., for our best optimized (BFP start) force field, are shown in Figure 6. Clearly, both the absorption and VCD are inadequately calculated. The major absorption peak occurs at 1220 cm^{-1} where experimentally we expect only a shoulder. This band correctly evidences positive VCD, but the large positive and negative VCD peaks found experimentally to higher energy are not at all adequately represented. Similarly, the experimentally found moderate absorption bands at 1450 and 1320 cm^{-1} are calculated to have little or no intensity with LMO model. The 1450-cm^{-1} VCD is correctly calculated to be small, although it does not evidence the monosignate nature seen experimentally and in the FPC-D result. However, the overall calculated LMO VCD and absorption magnitudes are within a factor of 5 of the average experimental values. While ϵ and $\Delta\epsilon$ are generally too large, the $\Delta\epsilon/\epsilon$ values calculated (such as for the 1250- and 1130-cm^{-1} bands) are again too small.

Discussion

These experimental and theoretical results constitute the first direct application of the FPC and LMO models to mid-IR VCD. The FPC results with optimized force fields provide surprisingly good qualitative reproduction of the experimental spectra. In the C–H and C–D stretching regions, both the FPC and LMO models gave equivalent qualitative results, and the effect of force field was one of shifting frequencies. Here the FPC results are clearly superior to those of the LMO, and the various force fields used yield significantly different results for both the entire spectral envelope and the rotational and dipolar strengths of individual modes. This force field dependence is undoubtedly due to differences in internal coordinate mixing caused by the off-diagonal terms added in the BFP force field.

The mid-IR is a stronger test than is the C–H stretching region of the quality of force field for two reasons: one, the modes in the mid-IR are less anharmonic than those in the C–H stretching region, and two, the mid-IR evidences mixing of many types of internal coordinates. The fact that the two optimized force fields (B and D) gave a much better representation of the spectra is evidence of the need for quality force fields in VCD calculation. In the mid-IR such optimization has significant effects upon the character of a normal mode in addition to improving the representation of its absolute frequency. On the contrary, in the C–H stretching region, little variation was seen between the various force fields, because optimization, at least for this molecule, does not significantly alter the character of these normal modes.

Examples of this force-field effect in the mid-IR can be seen by comparison of Tables I and II. These tables are arranged to facilitate comparison of similar modes, but the alignment is not perfect due to mixing of internal coordinates. Our calculations indicate that the CH_2 scissor and CHD scissor-like modes can roughly be characterized as local modes (like the C–H stretches). Their FPC calculated VCD is very similar at least among the force fields B, C, and D. This leads to a fairly easily interpretable VCD. The CH_2 scissors form coupled oscillators of opposite sense in each conformer. Thus, as expected, their VCD's cancel out and a small signal remains. The pair of CHD scissor-like modes do not form mirror images in the two conformers and hence the result of their coupling does not cancel with the result that the large VCD couplet is seen at 1280–1350 cm^{-1}. Here we see in the FPC-D results that the CHD coupling in the axial conformer dominates the observed VCD due to the very small splitting of these modes in the equatorial conformer. A similar effect occurs in the FPC-B results but not in FPC-C although the rotational strength sign pattern is preserved. These modes are examples of improved prediction of VCD for characteristic local modes, through better representation of frequency distribution, as noted earlier for the C–H stretching region.[6]

The next major VCD features lie in the 1200–1250 cm^{-1} region. Comparison of Tables I and II shows considerably less parallelism of calculated magnitudes and signs for the more mixed modes contributing to these bands. Here, variation of the sign of the rotational strength for a given mode is apparent when a change of force field is made, with the natural consequence that the line shape varies substantially between the force fields.

A third point to note is that the low-energy modes should vary substantially between force fields due to different assignments used in their optimization. For example, in force fields A and B a C_4H_8 A_1 rocking mode was assigned to ~750 cm^{-1},[14] but in C and D

Table I. Calculated Frequencies and Dipolar and Rotational Strengths for *trans*-(1*R*,2*R*)-Dideuteriocyclobutane for Early Force Fields[a]

no.	FPC-A[b]			FPC-B[c]			LMO-B[c]		symmetry and approximate description for force field B[d]	
	ν	D	R	ν	D	R	D	R		
					Equatorial Conformer					
1	1403	4.86	−2.59	1462	7.57	−9.67	0.23	−0.16	A	CH_2 scissor
2	1401	6.10	6.84	1451	9.98	9.80	0.22	0.28	B	CH_2 scissor
3	1262	1.33	19.07	1307	14.03	25.47	0.00	−0.51	A	CHD scissor-like
4	1251	0.07	−3.88	1301	14.15	−28.35	0.05	−0.94	B	CHD scissor-like
5	1277	2.15	−20.84	1266	2.05	2.42	0.57	1.70	B	wag + twist
6	1177	26.80	−45.74	1249	7.41	−12.39	0.95	−3.05	A	wag + twist + ring def
7	1235	0.11	−4.02	1221	1.93	−28.83	0.63	−15.41	A	twist + wag
8	1186	19.53	49.23	1226	7.44	58.20	1.37	22.03	B	twist + wag
9	1203	0.07	−0.32	1237	2.36	−9.29	0.34	−2.99	A	wag + twist + ring def
10	694	0.67	−3.67	714	0.02	−1.12	0.79	3.88	A	rock + twist
11	1175	4.02	7.84	1177	0.04	−1.05	0.00	−0.03	B	twist
12	1004	0.58	1.25	999	0.20	0.09	0.00	−0.02	A	ring breath
13	993	0.32	−0.29	1006	1.01	7.49	0.22	3.66	A	ring def + twist + wag
14	1014	3.55	−11.67	1033	1.84	−13.58	0.25	−4.76	B	ring def + twist + wag
15	875	0.15	−0.87	907	0.18	−0.48	0.01	0.19	A	ring def
16	981	1.02	4.30	980	0.50	−0.99	2.80	0.16	B	ring def
17	755	11.63	−12.24	835	5.95	−13.57	0.29	−1.62	B	ring def + wag + rock
18	745	10.28	17.59	821	5.40	15.73	0.38	2.74	A	ring def + wag + rock
19	634	10.39	−2.99	702	3.69	−1.36	2.11	−9.35	B	rock + twist
20	586	0.14	4.26	649	0.07	1.86	1.23	5.34	A	rock + twist
21	536	17.21	−1.23	563	22.54	−0.26	0.93	−0.91	B	rock
22	191	0.00	0.00	186	0.00	0.00	0.00	−0.01	A	ring pucker + rock
					Axial Conformer					
1	1404	4.44	5.96	1462	7.39	5.21	0.19	0.81	A	CH_2 scissor
2	1402	6.03	−6.57	1451	10.11	−6.23	0.25	−0.85	B	CH_2 scissor
3	1273	0.04	−3.44	1308	11.14	48.97	0.06	−2.10	A	CHD scissor-like
4	1268	1.50	5.53	1290	10.84	−62.81	0.08	1.82	B	CHD scissor-like
5	1295	0.00	0.49	1296	0.41	8.01	0.00	0.28	B	wag + twist
6	1220	3.23	−13.16	1251	11.86	−14.55	1.02	−5.10	A	wag + twist + ring def
7	1180	23.19	−45.86	1248	14.89	22.89	0.76	6.51	A	wag + twist + ring def
8	1192	1.13	1.20	1241	1.38	−3.88	0.01	−1.38	B	twist + wag
9	1203	6.25	23.90	1187	0.78	12.95	1.16	−15.99	A	twist + wag
10	1188	21.66	28.95	1214	0.48	−9.65	0.66	12.29	A	wag
11	701	1.09	−4.19	716	1.37	−7.34	1.00	−3.02	B	rock + twist
12	1029	2.10	14.01	1043	0.27	6.26	0.26	5.23	A	ring def + wag + twist
13	995	0.01	0.04	988	0.06	−0.06	0.19	0.62	A	ring breath
14	844	1.74	−4.61	901	1.80	−3.48	0.01	−0.05	B	ring def
15	946	0.33	−7.97	980	0.35	−2.94	0.17	−2.01	A	ring def + wag + twist
16	1008	0.00	−0.03	999	0.47	1.33	2.92	−1.30	B	ring def
17	746	6.46	14.40	810	1.55	8.41	0.03	−1.21	B	ring def
18	761	9.56	−12.30	836	3.92	−12.80	0.00	−0.06	A	ring def + wag
19	632	12.91	17.80	697	7.12	19.92	2.37	9.74	B	rock + twist
20	583	2.86	−19.69	647	1.82	−11.05	1.31	−6.27	A	rock + twist
21	530	15.84	5.96	555	19.95	1.31	1.12	0.89	B	rock
22	190	0.00	0.04	185	0.00	0.03	0.00	0.00	A	ring pucker + rock

[a] In FPC calculations, empirical charges were used with −0.28 |e| on C and +0.14 |e| on H(D) atoms; frequencies are in cm^{-1}, dipolar strengths in 10^{-39} (esu·cm)^2 and rotational strengths in 10^{-44} (esu·cm^2). [b] L&N force field; see text. [c] L&N force field refined further; see text. [d] Inferred from diagonal force constants with potential energy distribution greater than 10%.

this was reassigned to 1153 cm^{-1}.[8] Hence, the basic character of modes below 1100 cm^{-1} will differ between the force fields. This is indicated by comparison of Tables I and II. Due to this and the low signal-to-noise ratio found, little can be made of the agreement or lack of it for the weak bands in the lower energy region.

The FPC model is an empirical, parameterized theory whose parameters are the charges. Here we have succeeded qualitatively by using charges transferred from our near-IR studies. However, the quantitative aspects of this approach are not good. Absorption and VCD are overestimated by at least an order of magnitude. This simply means that the charge parameters used in the mid-IR should be rescaled. In fact, this will make them more physically reasonable as can be seen from the FPC-D CNDO charge results. Here while the absorbance and VCD are calculated to be small, in comparison with experiment, they are within an order of magnitude. In other words, re-parameterized charges of ca. −0.05 |e| on carbon and 0.025 |e| on hydrogen may be more realistic for the mid-IR. However, the $\Delta A/A$ values will not be changed by such re-parameterization. For the 1330-cm^{-1} VCD couplet, the FPC-D $\Delta A/A$ value is too low by a factor of $\sim$5. This may be a true indication of weakness in the FPC model. Proper representation of line width and overlap may also be a factor here. It can be noted that the C–H stretches are more anharmonic than the modes in the mid-IR. This might be a cause for the large experimental dipolar strengths for C–H stretches which, in turn, would have necessitated the unusually large "charge" parameters used to describe the C–H stretching absorption spectrum.

The need for scaling emphasizes the parametric nature of the charges. Our experience implies that one should use smaller parameters, as compared to the C–H stretch values, to best represent the mid-IR spectra. (In heteroatom containing molecules this may not be true.) The variability of "charge" magnitudes underlines the fact that they have no physical meaning beyond an empirical description of the IR intensity. This also makes "charge" selection for molecules with heteroatoms or more complex structural units quite difficult.

The relative failure of the LMO model is perhaps more surprizing than the success of the FPC. It has been suggested[19] that due to the ring nature of these compounds the localization procedure has difficulties. If this is true, the success found in the C–H stretching region for this and other ring molecules[5] may not

(19) Polavarapu, P. L., private communication.

Table II. Calculated Frequencies and Dipolar and Rotational Strengths for *trans*-(1*R*,2*R*)-Dideuteriocyclobutane for BFP and Optimized Force Fields[a]

	FPC-C[b]			FPC-D[c]			FPC-D-CN[c]		LMO-D[c]			
no.	ν	D	R	ν	D	R	D[a]	R[a]	D	R		symmetry and approximate description for force field D[d]
							Equatorial Conformer					
1	1486	5.56	−6.36	1459	8.09	−10.14	2.73	−24.00	0.14	−0.10	A	CH_2 scissor
2	1466	8.18	5.93	1451	9.55	8.97	7.42	23.29	0.14	0.21	B	CH_2 scissor
3	1342	5.55	16.30	1310	10.54	25.27	2.63	−8.99	0.03	−1.26	A	CHD scissor-like
4	1317	3.39	−18.04	1309	11.27	−30.66	4.12	14.64	0.03	1.06	B	CHD scissor-like
5	1270	10.33	−12.55	1252	2.23	−3.53	4.23	−23.23	0.36	−3.28	B	wag + twist + scissor
6	1248	17.16	−4.79	1234	0.25	1.24	0.42	1.93	0.03	0.36	A	twist + wag + ring stretch
7	1215	3.16	−37.57	1216	8.11	−60.27	1.04	−7.78	2.10	−24.11	A	wag + twist + rock
8	1211	12.78	70.08	1214	10.56	65.43	1.69	8.94	2.31	24.03	B	wag + twist
9	1204	0.00	0.30	1206	6.45	17.20	6.98	25.82	0.71	5.49	A	wag + twist + ring stretch
10	1141	3.29	−2.30	1124	0.83	−0.21	0.00	0.00	0.02	−0.13	A	rock + ring stretch
11	1107	1.54	−11.28	1060	1.37	−12.80	1.33	−8.68	0.30	−3.70	B	wag + ring stretch + twist
12	1038	0.29	2.53	982	0.00	0.22	0.00	0.12	0.08	1.05	A	ring stretch + twist + wag
13	977	1.66	4.30	968	1.62	4.25	0.00	−0.17	0.08	0.36	A	ring stretch + rock
14	923	1.04	−0.01	923	0.74	−1.54	0.27	1.47	0.01	0.26	B	twist + wag + ring stretch
15	913	0.37	−1.11	914	0.63	−1.45	0.50	0.65	0.01	0.23	A	ring stretch
16	854	8.17	−15.53	869	9.65	−15.33	4.02	−10.15	0.95	−3.27	B	rock + ring bend + twist + ring stretch
17	783	4.07	−3.19	798	4.83	−1.28	3.49	−0.26	0.65	−0.36	B	ring stretch + ring bend + twist + wag
18	776	5.60	14.43	795	6.08	16.43	0.33	5.35	0.72	3.58	A	wag + ring stretch + rock + twist
19	677	1.35	−5.81	682	1.17	−0.02	11.83	29.29	2.41	−6.87	B	rock + twist + ring bend
20	668	0.21	5.28	669	0.02	−1.43	13.14	−30.13	1.48	7.19	A	rock + twist + ring stretch
21	566	20.63	−0.41	585	19.05	−0.14	18.25	2.15	3.41	−0.83	B	rock + ring bend
22	113	0.00	−0.00	186	0.00	0.00	0.00	0.03	0.00	−0.00	A	ring pucker + rock
							Axial Conformer					
1	1486	5.72	2.76	1459	7.58	6.59	2.50	21.27	0.14	0.47	A	CH_2 scissor
2	1466	8.32	−6.13	1451	10.08	−7.56	7.33	−25.88	0.17	−0.50	B	CH_2 scissor
3	1337	4.64	23.45	1327	8.38	36.59	3.57	36.96	0.07	−1.73	A	CHD scissor-like
4	1308	3.79	−18.63	1295	6.73	−44.19	7.78	−38.52	0.19	3.05	B	CHD scissor-like
5	1272	21.71	−15.28	1257	0.39	8.14	0.26	13.66	0.14	0.42	B	wag + twist
6	1275	19.12	−16.09	1251	12.51	−39.51	12.86	−41.08	0.56	−7.96	A	wag + twist + ring stretch
7	1251	1.32	25.94	1246	17.21	29.48	16.63	31.39	0.52	5.69	A	wag + twist + ring stretch
8	1213	2.01	24.32	1220	2.71	21.46	0.29	0.69	1.53	13.30	B	wag + twist + ring stretch
9	1129	2.11	−27.35	1131	2.40	−17.74	1.15	−7.79	2.03	−19.05	A	twist + wag + scissor + ring stretch
10	1179	0.02	0.17	1124	0.00	0.00	0.00	0.00	0.00	0.00	A	wag + twist
11	1127	0.55	2.62	1080	0.67	6.75	1.86	10.42	0.02	−0.62	B	rock + ring stretch
12	1025	0.08	2.87	1023	0.00	0.43	0.02	−0.43	0.42	4.26	A	ring stretch + twist + rock + wag
13	990	0.04	−0.02	987	0.07	−0.22	0.60	1.03	0.26	0.92	A	ring stretch
14	915	2.15	−7.12	913	2.51	−5.40	0.45	−3.22	0.01	−0.14	B	ring stretch
15	904	3.97	8.79	901	5.50	2.84	1.22	7.92	0.14	0.91	A	ring stretch + twist + wag + rock
16	877	6.96	−0.75	885	7.68	1.61	5.92	−1.78	0.97	−0.27	B	ring bend + rock
17	807	3.35	9.07	807	4.13	10.70	3.37	−0.67	0.08	1.51	B	ring stretch + wag
18	783	1.44	−9.84	773	1.34	−12.46	5.54	−5.94	0.28	0.32	A	twist + wag + rock + ring stretch
19	674	6.12	22.56	680	4.85	19.82	5.95	−20.75	2.52	7.65	B	rock + twist + wag
20	656	3.93	−22.61	668	2.87	−17.88	6.38	23.13	2.13	−8.99	A	rock + twist
21	531	16.28	1.40	551	14.93	0.75	12.37	−0.38	3.52	0.53	B	rock + ring bend
22	112	0.00	0.01	187	0.00	0.03	0.00	−0.01	0.00	0.00	A	ring pucker + rock

[a] In FPC-C and FPC-D, empirical charges as in Table I were used, but in FPC-D-CN, CNDO charges with −0.0189 |e| on C, +0.0171 |e| on equatorial H(D), and +0.0018 |e| on axial H(D) atoms were used. Frequencies are in cm^{-1}, dipolar strengths in 10^{-39} (esu·cm)^2, and rotational strengths in 10^{-44} (esu·cm)^2 except for FPC-D-CN whose dipolar and rotational strengths are given respectively in 10^{-41} and 10^{-46} (esu·cm)^2. [b] BFP ab initio scaled force field; see text. [c] BFP force field optimized further; see text. [d] Inferred from diagonal force constants with potential energy distribution greater than 10%.

be affected by such consideration. Since the C–H bonding orbitals are probably well-localized as compared to the ring orbitals, it may be reasonable to observe success in one region but not in the other with the LMO model. In fact, we had originally expected that the FPC model would have difficulties in the mid-IR for virtually the same reasons. At present there is insufficient data to judge the question of the ultimate utility of the LMO model for the mid-IR.

The inverse question can also be raised: is the success of the FPC model here an accident? Again, since this is the first such mid-IR study, we cannot say with certainty. However, intuitively, we expect that the FPC has in it one element of the true physical basis for VCD, and to the extent that this aspect of mechanism is dominant, the FPC will more-or-less correctly represent the observed VCD. The crucial problem is to decide for which molecules the "FPC-like" part might be dominant. In saturated hydrocarbons with no heteroatoms it is reasonable to expect that we have the best chance of seeing the charge motion strongly correlated with nuclear motion and hence the best chance of FPC success. Our study bears this out.

Another aspect to this comparison is also worth consideration. It could be possible that the many factors left out of the FPC model such as charge flow, polarizability effects, and vibronic coupling tend to cancel out for this molecule. Thus correcting one aspect of this model, as may be done in the LMO scheme, could upset the FPC's balance.

Conclusion

We have presented the first detailed comparison of FPC and LMO calculated VCD in the mid-IR with experimental spectra. It is seen that, for *trans*-1,2-dideuteriocyclobutane, the FPC model gives satisfactory results. Contrary to our experience with near-IR VCD, the calculated spectra were quite sensitive to force field, and the LMO model gave qualitatively worse results. We interpret these results as more indicative of the applicability of the FPC model to saturated hydrocarbons than as evidence for the general usefulness of the model. Such a determination would necessitate systematic study of well-characterized compounds of different

structural types. This work is underway in our and other laboratories.

Acknowledgment. We thank the National Science Foundation (CHE 81-04997) and the National Institutes of Health (GM-30147) for support of this work and Prof. P. L. Polavarapu for use of his LMO program. T.A.K. thanks Prof. K. L. Kompa and the Max-Planck-Institut für Quantenoptik for hospitality during the time when this paper was being written and the Fulbright Foundation for support.

Registry No. *trans*-1,2-Dideuteriocyclobutane, 75156-31-9.

Relative Electron Affinities of Substituted Benzophenones, Nitrobenzenes, and Quinones

Elaine K. Fukuda and Robert T. McIver, Jr.*

Contribution from the Department of Chemistry, University of California, Irvine, California 92717. *Received June 20, 1984*

Abstract: The relative electron affinities of 53 molecules have been determined by measuring equilibrium constants for gas-phase electron-transfer reactions of the general type $A^{-\cdot} + B = B^{-\cdot} + A$. A pulsed ion cyclotron resonance (ICR) spectrometer was utilized to generate, store, and detect molecular anion radicals at pressures below 1×10^{-5} torr. The ions were generated by electron capture and stored for several hundred milliseconds in a one-region ICR analyzer cell. A scale of relative electron affinities has been constructed by using the method of multiple overlaps. Substituent effects on the electron affinities of various nitrobenzenes, benzophenones, and quinones are discussed.

Chemical reactions involving negative ions are ubiquitous. For example, the primary source of visible light from the sun results from radiative electron attachment to hydrogen atoms.[1] In the earth's atmosphere, negative ions such as O^-, Cl^-, and NO_2^- play an important role in the chemistry of the ionsphere.[2] Many reactions in solution are being interpreted in terms of the single-electron-transfer (SET) mechanism.[3] And it is well-known that such biologically important processes as photosynthesis and oxidative phosphorylation involve electron-transfer reactions.

One of the fundamental properties of a gaseous negative ion is the lowest energy required to remove an electron. This energy is called the electron affinity (EA) and is equal to ΔE for the process

$$A^- = A + e^- \quad (1)$$

where both the ion and neutral are gaseous species in their ground electronic, vibrational, and rotational states, and the electron has zero kinetic and potential energy. The quantity EA is positive if a stable negative ion exists.

Many experimental methods have been developed for measuring electron affinities.[4] Photodetachment and photoelectron spectroscopy (PES) are optical methods which study the reaction

$$A^- + h\nu \rightarrow A + e^- \quad (2)$$

In the photodetachment experiment, ion abundance is monitored as a function of varying wavelength to determine the threshold for photodetachment,[5,6] while in photoelectron spectroscopy a fixed frequency light source intersects a beam of negative ions and the resultant photoelectrons are energy-analyzed.[7]

Another approach involves observing the occurrence of ion–molecule charge-transfer reactions such as

$$SH^- + NO_2 \rightarrow NO_2^- + SH \quad (3)$$

Since this is a fast reaction at thermal energies, it is safe to conclude that the $EA(NO_2)$ is greater than EA(SH). Exothermic charge-transfer reactions have been studied with flowing afterglow systems[8] and ion cyclotron resonance spectrometers.[9,10] Another approach involves the use of tandem mass spectrometers[11] and alkali atom beam instruments[12,13] to study the translational energy dependence for endothermic electron-transfer reactions.

The gas-phase acidity scale has been used to calculate the electron affinities of several radicals.[14-16] Equilibrium constants for reactions of the type

$$F^- + AH = A^- + HF \quad (4)$$

(1) Wildt, R. *Astrophys. J.* **1939**, *89*, 295.
(2) Ferguson, E. E.; Fehsenfeld, F. C.; Albritton, D. L. In "Gas Phase Ion Chemistry"; Bowers, M. T., Ed.; Academic Press: 1979; Vol. 1, Chapter 2.
(3) For example, see: (a) Amatore, C.; Pinson, J.; Saveant, J.-M.; Thiebalt, A. *J. Am. Chem. Soc.* **1981**, *103*, 6930. (b) Guthrie, R. D.; Cho, N. S. *J. Am. Chem. Soc.* **1979**, *101*, 4698. (c) Klinger, R. J.; Mochida, K.; Kochi, J. K. *J. Am. Chem. Soc.* **1979**, *101*, 6626.
(4) For recent reviews of electron affinities see: (a) Janousek, B. K.; Brauman, J. I. In "Gas Phase Ion Chemistry" ; Bowers, M. T., Ed.; Academic Press: New York, 1979; Vol. 2, p 53. (b) Corderman, R. R.; Lineberger, W. C. *Annu. Rev. Phys. Chem.* **1979**, *30*, 347.
(5) Branscomb, L. M. In "Atomic and Molecular Processes"; Bates, D. R., Ed.; Academic Press: New York, 1962; p 100.
(6) Smyth, K. C.; Brauman, J. I. *J. Chem. Phys.* **1972**, *56*, 1132.
(7) Lineberger, W. C. In "Chemical and Biochemical Applications of Lasers"; Moore, C. B., Ed.; Academic Press: New York, 1974; Vol. 1, p 71.
(8) Dunkin, D. B.; Fehsenfeld, F. C.; Ferguson, E. E. *Chem. Phys. Lett.* **1972**, *15*, 257.
(9) Fukuda, E. K.; McIver, R. T., Jr. *J. Chem. Phys.* **1982**, *77*, 4942.
(10) Rains, L. J.; Moore, H. W.; McIver, R. T., Jr. *J. Chem. Phys.* **1978**, *68*, 3309.
(11) Lifshitz, C.; Tiernan, T. O.; Hughes, B. M. *J. Chem. Phys.* **1973**, *59*, 3182.
(12) (a) Nalley, S. J.; Compton, R. N. *Chem. Phys. Lett.* **1971**, *9*, 529. (b) Nalley, S. J.; Compton, R. N.; Schweinler, H. C.; Anderson, V. E. *J. Chem. Phys.* **1973**, *59*, 4125.
(13) Leffert, C. B.; Jackson, W. M.; Rothe, E. W.; Fenstermaker, R. W. *Rev. Sci. Instrum.* **1972**, *43*, 917; (b) Leffert, C. B.; Jackson, W. M.; Rothe, E. W. *J. Chem. Phys.* **1973**, *58*, 5801.
(14) Bartmess, J. E.; Scott, J. A.; McIver, R. T., Jr. *J. Am. Chem. Soc.* **1979**, *101*, 6046.
(15) Bartmess, J. E.; Scott, J. A.; McIver, R. T., Jr. *J. Am. Chem. Soc.* **1979**, *101*, 6056.
(16) Bartmess, J. E.; McIver, R. T., Jr. In "Gas Phase Ion Chemistry"; Bowers, M. T., Ed.; Academic Press: New York, 1979; Vol. 2, Chapter 11.

0002-7863/85/1507-2291$01.50/0